

33 After centuries of base metal and silver mining, the open pit and underground iron ore (limonite
34 and siderite) mining of Rudabánya (Silicicum stratigraphic superunit, Lower-Middle Triassic, NE
35 Hungary) went on from 1872 until 1985. Approximately 38 Mt of iron ore was excavated during
36 this period, the recent geological resource exhibits 43 Mt of low grade iron ore (including limonite,
37 siderite and ankerite with an average Fe content of 23.5 wt. %, and siliceous siderite) (Balla et al.
38 1987).

39 Similar iron ore deposits occur in the Alps-Carpathian region. In the Tethyan Realm the Triassic-
40 Middle Jurassic was an important epoch of Fe mineralization (Hurai 2005). Fe deposits with
41 variable reserves are distributed from Slovenia to Austria and Slovakia. The Silicicum unit was part
42 of the European Continental Margin (continental margin of the Mesozoic Tethys) at that time. The
43 siderite–sulphide veins and siderite replacement deposits of the Gemericum in Slovakia represent
44 one of the largest accumulations of siderite in the world, with approximately 160 Mt of mineable
45 FeCO₃ ore. Carbonate-replacement siderite deposits of the Gemericum hosted by a Silurian
46 limestone belt are similar to stratabound siderite deposits of the Eastern Alps (e.g. Erzberg, Austria;
47 Radvanec et al. 2004). The siderite–sulphide veins and siderite replacement deposits were classified
48 as metamorphogenic, they were formed during several stages of regional crustal-scale fluid flow
49 (multistage hydrothermal circulation via Variscan and Alpine mineralization phases) (Radvanec et
50 al. 2004). The Ljubija siderite deposit in the Dinarides (Bosnia-Herzegovina) represent also
51 hydrothermal–metasomatic Fe mineralization. Here the iron ore occurs as stratabound siderite and
52 ankerite replacement-type bodies in limestones and as siderite-sulphide veins within shales.
53 Superimposed Alpine retrograde metamorphic fluids were observed and might well be compared to
54 the fluids linked to the formation of the Rudňany deposits in Gemericum. The potential resources of
55 iron ore in the Ljubija district have been estimated to 500 Mt with 40 to 49 wt. % Fe (Palinkaš et al.
56 2008).

57 The renewed exploration of the Rudabánya ore deposit began in 2007 and it is resulted in the
58 delimitation of newly recognized Fe, Pb, Zn, Ag and Cu enrichments and the determination of their
59 formation. The additional aim of this work was to clarify the paleo-environmental conditions, trace
60 the possible metal source and prepare an ore formation study of the Lower Triassic Bódvaszilas
61 Sandstone Formation (BSF) which includes a previously un-mined sub-grade iron ore (local name
62 is „siliceous sparry iron ore” or „creamspar”).

63 During the investigation of this iron ore signs of microbial mediation were observed, which
64 were formerly unknown in these rocks. This has initiated new investigations and as a result a new
65 ore formation model was built up.

66

67 **2. Geological setting**

68

69 The Rudabánya iron and base metal deposits are hosted by Lower-Middle Triassic siliciclastic
70 formations and carbonates which are located in the Aggtelek-Rudabánya Mts. in NE Hungary, in
71 the Silicicum stratigraphic superunit of the Alps–Carpathians–Pannonian (ALCAPA) region (Fig.
72 1a). The Silicicum stratigraphic unit built up from Upper Permian – Lower Triassic evaporites
73 (Perkupa Evaporite Formation), Lower Triassic siliciclastic formations and carbonates (Bódvaszilas
74 Sandstone, Szin Marl, Szinpetri Limestone – tidal flat and shallow marine ramp facies) and Middle-
75 Upper Triassic and Jurassic carbonates (Gutenstein Formation, Steinalm Formation, Dunnatető
76 Limestone, Bódvalenke Limestone, Hallstatt Limestone – carbonate platform and basin facies)
77 (Szentpétery & Less 2006) (Fig. 1b).

78 The later NNW-SSW striking main faults of the so-called Darnó Structural Zone divide the
79 mineralized area into 100-1000 m wide slabs with differently structured paleozoic-mesozoic
80 sequences (Fig. 1c). The Rudabánya ore deposit complex, is located in the most uplifted, 0.3-3 km
81 wide central zone in the axis of the Darnó Zone. It consists of separate siderite blocks (> 1000

82 blocks) which are of carbonate and siliciclastic rocks in a tectonised clayey matrix (Pantó 1956;
83 Hernyák 1967; Szentpétery & Less 2006; Földessy et al. 2010). The sizes of the lenticular-blocky
84 siderite bodies are variable, their length varies between 60-600 m, their width between 10-100 m,
85 their thickness are between 3-100 m (Kun 1989).

86 Previously several ore-forming models were built up about the iron mineralization of
87 Rudabánya, some of them assumed magmatic origin (Nagy 1982; Balla et al. 1987). According to
88 another scenario magmatism was not necessary to the iron ore formation, but the mixing between
89 the pore waters of the Permian-Lower Triassic siliciclastic succession and the fissure waters of the
90 Triassic carbonates were proposed (Csalagovits 1973; Fügedi et al. 2010).

91 According to the latest studies the Rudabánya ore deposit complex was formed in several
92 periods. Three main deformation phases divided temporally the periods of ore formation (Földessy
93 et al. 2010; Németh et al. 2013). A synsediment, stratiform, sedimentary-exhalative Pb-Zn-barite
94 accumulation was formed in the pelitic and carbonatic, reductive Szin Marl as the earliest ore
95 forming phase. A later metasomatism (probably of Cretaceous age) has introduced the siderite ores
96 (local name is „sparry iron ore”) hosted by the Lower-Middle Triassic Szinpetri Limestone,
97 Gutenstein Dolomite and the un-mined sub-grade iron ore of Bódvaszilás Sandstone. In the third
98 ore forming phase (related to Darnó Zone formation, probably of Paleogene age) mainly pyrite-
99 bearing massive sulphide filled veins, and later Pb-, Zn-, Ag- and Cu-enrichments with barite were
100 generated. The faults of the Darnó Zone promoted the latest, a probably low temperature sulphidic
101 ore formation (As-, Sb-, Hg- and Ag-enrichments). In this last stage of the ore formation the
102 siderite-base metal ore formations were exhumed and oxidized near the surface, and a limonitic
103 zone and secondary enrichments (native copper, malachite, cerussite, anglesite, smithsonite) were
104 formed by subsurface solutions (Földessy et al. 2010). At the basis of the Miocene beds
105 sphaerosideritic iron ore was also formed (Szakáll 2001).

106

107 3. Samples and methods

108

109 Representative samples of Bódvaszilas Sandstone (87) and siliceous sparry iron ore
110 (creamspar, 20) were investigated from the Rudabánya open pit and from a surface outcrop in
111 Rudabánya, and samples from Bódvaszilas Sandstone from the non-mineralized area (Aggtelek
112 Mts.) were also collected (Fig. 1b).

113 The Bódvaszilas Sandstone samples are blueish-greyish green, locally red colored rocks.
114 These are mainly grain-supported, well sorted, very fine- and rarely fine-grained quartzarenites and
115 matrix-supported, well sorted, oligomict siltstones and claystones. The pale yellow „siliceous sparry
116 iron ore” occurs as pore- and vein-fillings in the Bódvaszilas Sandstone and as massive ore in the
117 transitional layers of the Bódvaszilas Sandstone and the overlying Szin Marl Formation.

118 Detailed macroscopic and microscopic petrographic investigations were done first to acquire
119 information before other analyses (NIKON ECLIPSE 600 rock microscope, Institute for Geological
120 and Geochemical Research, Budapest, Hungary). X-ray powder diffraction (XRD) of bulk rock
121 samples for mineralogy was performed on a Bruker D8 Advance diffractometer (CuK α source, 40
122 kV, 40 mA, secondary graphite crystal monochromator, scintillation detector) at the Institute of
123 Mineralogy and Geology, University of Miskolc, Hungary.

124 Electron microprobe analyses were done by the means back-scattered electron imaging (BSE)
125 and energy dispersive spectrometry (EDS) for main and trace element distribution on a JEOL JXA-
126 8600 Superprobe (15 kV, 20 mA, carbon coating, 60 s acquisition time) at the same institute.

127 The $^{13}\text{C}_{\text{carb}}$ and $^{18}\text{O}_{\text{carb}}$ stable isotopic analyses on siliceous sparry iron ore and total organic
128 carbon analysis on siliceous sparry iron ore and the host siliciclastic succession were carried out
129 bulk samples at the Institute for Geological and Geochemical Research and in the Geographical
130 Institute, Research Centre for Astronomy and Earth Sciences, Hungarian Academy of Sciences,
131 Budapest, Hungary.

132 Chemical analyses (major, trace and rare earth element) were made on Bódvaszilas Sandstone
133 samples by ICP-MS and ICP-AES (ALS Chemex laboratories, Vancouver).

134

135 **4. Results**

136

137 **4.1. Petrological and microtextural characteristics of Bódvaszilas Sandstone Formation**

138

139 The Bódvaszilas Sandstone is a mature sediment based on the quantity and quality of the grains.
140 The absence of unstable grains like polycrystalline quartz and lithic fragments, and the low quantity
141 of feldspars are typical. The most frequent clastic constituent is monocrystalline quartz (approx. 85
142 %) and muscovite (10 %) by visual estimation. In low quantity other types of mica (altered
143 phlogopite, biotite) may be present. The accessory minerals are zircon, apatite, rutile and monacite,
144 rarely xenotime, schorl and ilmenite. As opaque mineral only disseminated, euhedral, rarely
145 framboidal pyrite occurs commonly along the fractures and laminae. In the matrix of the formation
146 chlorite (clinochlore), illite, and very rarely kaolinite and fine, dispersed hematite flakes occur.

147 The cement between the grains is built up from quartz and a large amount of carbonate
148 (creamspar). The three types of the pale yellow carbonate are the following:

149 1. Small nests (diameter 1-5 mm) between the grains as the cement of the siliciclastic
150 formation. The pore-filling nests or patches are present in the coarser grained sections (fine-grained
151 sandstone). Where the rock is more compact, the abundance of this carbonate is less. In the pore-
152 filling cement of the Bódvaszilas Sandstone and at the contact of the grains and the cement, both in
153 Rudabánya and in the Aggtelek Mts. fine filamentous, pearl necklace-like microbial microtexture
154 (mineralized microbially produced texture – MMPT) is widely prevalent (Fig. 2a,c,f). These
155 textures often form colonies. Between the grains the clay minerals are very common.

156 2. Pore-filling creamspar in 1-2 cm wide veins crosscutting layering. At the margin of the
157 sandstone and the vein coarse-grained, euhedral quartz is present.

158 3. In the upper part of the Bódvaszilas Sandstone, in the transition layers to the Szin Marl,
159 several centimeters thick, contiguous sections. These are massive syndimentary intercalations.
160 Euhedral-subhedral quartz with sparse hematite flakes may be connected to the coarse grained
161 (even 1 mm) sparite carbonate crystals. In the massive carbonate sections coarse-grained (even 0,5-
162 1 mm) euhedral quartz crystals are also present (megacrystals, Scholle & Ulmer-Scholle 2003),
163 occasionally a thin border line suggests the original quartz grain. In the massive carbonate sections
164 and in the vein-filling carbonate along the cleavage faces of the sparite crystals, in negligible
165 quantity, filamentous MMPT textures can also be observed (Fig. 2b). In the carbonate very rarely
166 red colored clasts with pyrite, quartz and hematite are present.

167 The formation is compacted and the slightly lineated texture and the concavo-convex and
168 rarely sutured grain contacts can be observed with dissolution at the margin of the grains, and the
169 synthaxial quartz overgrowths on monocrystalline quartz grains. The authigenic quartz engulfs and
170 replaces the pore-filling carbonate cement. Occasionally the remnants of the carbonate cement as
171 inclusions can be found in the quartz cement.

172

173 **4.2. Mineralogy (XRD) of siliceous sparry iron ore**

174

175 By XRD peaks of the R-3c space-group were observed, with $d(\text{\AA})$ values as intermediary
176 between siderite and magnesite structure. The $d(104)$ varies between 2.76 \AA and 2.78 \AA , indicating
177 a larger range of substitutions. Intensities were affected by strong preferred-orientation, but
178 applying the March-Dollase correction, we obtained relative intensities characteristic for the siderite
179 lattice. The creamspar is usually accompanied by dolomite and quartz.

180

181 **4.3. Chemistry of carbonate by EPMA**

182

183 The chemical composition and crystal structure related properties of the creamspar from
184 Bódvaszilas Sandstone is described for the first time. The texture of the creamspar and its
185 composition is very similar in the three types (pore-filling cement, vein-fillings, massive carbonate
186 sections). According to our observations it often shows chemical zonation patterns, on the
187 rhombohedron faces (Fig. 2e). The creamspar is always inhomogeneous in elemental composition,
188 but it is always Fe- and Mg-rich carbonate with low Mn content (never pure siderite or pure
189 magnesite, it is always with excess substitution of Mg and Fe). The Fe and Mg ratio changes in
190 several micrometers level, it is independent of textural characteristics. In the analysed samples the
191 Fe content varies between 0.11 and 0.84, and the Mg content between 0.25 and 0.65 atoms in the
192 RCO_3 theoretical formula (R: Fe, Mg, Mn, Ca) (Fig. 3).

193

194 **4.4. C and O isotopic values of the carbonate**

195

196 The samples of the vein-filling and massive creamspar sections show negative C and O
197 isotopic values: $\delta^{13}\text{C}_{\text{PDB}}$: -6.18 ‰ - -3.91, the $\delta^{18}\text{O}_{\text{PDB}}$: -14.66 - -12.21 (‰).

198

199 **4.5. TOC values of the carbonate and the host rock**

200

201 The Total Organic Carbon content of the creamspar from the massive carbonate sections is
202 between 0.38-2.63 wt. %, and the host rock is between: 0.05-0.06 wt. %.

203

204 **5. Discussion**

205

206 Some representative samples were selected for paleoenvironmental study. The host rock of the iron
207 ore (BSF) was a mature, recycled sediment based on monomict mineral composition, derived from
208 an acidic source area according to the accessory minerals and the La/Th and La/Co ratios (Bhatia &
209 Crook 1986). Our observations reinforce the opinion of Kovács et al. (2004), that the source area
210 was the Permian molasse in the basement of the Gemericum.

211 According to the geochemical environmental indicators (Wignall & Meyers 1988; Rimmer 2004;
212 Yang et al. 2011) during the sedimentation and the early diagenesis oxic conditions were existed
213 (Table 1).

214 Between the grains of the BSF (host succession), in the pore-filling cement, at the margin of
215 the grains, and at the contact of the carbonate cement and the grains filamentous textures of
216 assumed microbial origin (MMPT) are present that often form microbial-like colonies. The
217 microbial fossils altered to goethite. Between the grains clay minerals are frequent (the gel-like
218 layer around the colonies of bacteria altered to smectite, Fig. 2d). The characteristic microbial
219 filaments along the cleavage faces of creamspar layers of the samples from Rudabánya were also
220 observed nevertheless in smaller quantity. MMPT are present in much less quantity in the non-ore
221 bearing distal basin area in the same formation (Aggtelek Mts., Bódvaszilás Sandstone Formation).

222 Several Fe (II) oxidizing microbes (FeOB) are known in shallow and deep marine
223 environment, some bacteria carry out autotrophic metabolism, i.e. they synthesize their cell
224 constituents from the inorganic materials of the environment. Four kinds of recent microbial Fe(II)
225 oxidizing metabolism are reported (Ehrlich 1990; Fortin 1997; Konhauser 1998). The microbial Fe
226 oxidizing processes are very effective (Ehrlich 1990). According to the mineralogy and the
227 morphological features the presence of suboxic, neutrophylic microbial forms are the most
228 probable. In suboxic, neutrophylic environment the Fe(II) oxidizing bacteria synthesize ferrihydrite
229 (hydrated ferric oxyhydroxide), which transform to more stable mineral forms like goethite or
230 hematite within a few months while quartz is segregating (Schwertmann & Cornell 2007). The iron-

231 oxide and the segregated quartz may form clay minerals (green clays, e.g. celadonite and/or
232 smectite). Similar clay formation occurred in our samples and was also mentioned by Hernyák
233 (1967).

234 The bacterial filaments are embedded in the pore-filling carbonate cement of Bódvaszilas
235 Sandstone and at the margin of the grains. This observation suggest a that prior to the formation of
236 creamspar there was not any intergranular cement (there are no residual cement), and the newly
237 formed cement did not compact significantly. An external Fe-bearing solution reached and
238 influenced this succession. It is possible that the microbes were present previously in the fluid-
239 saturated siliciclastic succession nevertheless the Fe-bearing solution may have also transported
240 them to the sediment. The microbes carried out autotrophic metabolism in order to gain energy.
241 This produced ferrihydrite with the oxidation of Fe(II) from the Fe-bearing solution (first microbial
242 cycle syn- to early diagenetic in suboxic neutrophylic environment). The ferrihydrite with the
243 practically inert quartz grains, and the pore-fluids and the organic matter of the died microbes had
244 formed an unstable system. As the organic matter is reactive, it reacted with the ferrihydrite which
245 led to siderite and ankerite formation with the contribution of microbes via heterotrophic
246 metabolism in suboxic to anaerob environment (Konhauser 1998). Additional ions in the Fe-bearing
247 solution (Ca^{2+} , Mg^{2+} , HCO_3^- , etc.) and the organic C may form other mixed carbonates (second
248 microbial cycle in suboxic/anoxic Eh, neutrophylic environment). The completeness of the process
249 depends on the ratio of the available phases thus goethitic-hematitic parts may remain. The C
250 isotope ratio of the forming carbonates is negative, which supports the mineralized organic C
251 content. The negative C isotope ratio and the remnant organic matter (0.05-2.63 wt. %) of our
252 samples also confirm the microbial contribution. The texture of the pore-filling creamspar is
253 misleadingly similar to the creamspar formed in the carbonate layers nevertheless the high
254 resolution optical microscopy explored textural features and differences, which highlight that the
255 ore formation went on different ways in the siliciclastic and carbonate host succession.

256 The low quantity of microbial traces in the massive creamspar sections suggests that in the
257 primarily carbonate host layers the creamspar probably generated not via microbial mediation but
258 metasomatism, as the texture and the element distribution is rather similar to the younger, dolomite-
259 hosted, metasomatic iron ores'. The zonation occurs occasionally by rhombohedron and completely
260 similar to the observed zonation (Pantó 1956; Szakáll 2001) of the mined sparry iron ore formed in
261 the Middle Triassic dolomites. The element exchange via metasomatism has moved forward
262 paralell to the rhombohedron faces which has caused the characteristic zonation. The $\delta^{13}\text{C}$ and $\delta^{18}\text{O}$
263 isotope values of the creamspar from the Bódvaszilas-Szin transitional layers and the sparry iron ore
264 samples from the Rudabánya open pit are similar to each other and the values are nearly the same as
265 the siderite (sparry iron ore) samples of Hofstra et al. (1999). The similar texture observed by SEM-
266 EDS and similar $\delta^{13}\text{C}$ and $\delta^{18}\text{O}$ values of the creamspar in the Bódvaszilas-Szin transitional layers
267 and the sparry iron ore suggest, that the two type of iron ore presumably formed by the same
268 process, i.e. metasomatism between the succession and a high Fe-bearing solution. It is possible that
269 in these sections some microbial Fe oxidation also occurred but its ratio to the metasomatism was
270 negligible.

271 The examination of the carbonate cement of the samples from the Aggtelek Mts. (non-ore-
272 bearing area) denotes that the Fe addition affected not only the Bódvaszilas Sandstone Formation of
273 Rudabánya but the similar formation in the Aggtelek Mts. although by less intensity. In the pore-
274 filling carbonate cement and at the margin of the grains the microbial filaments can be observed in
275 the Bódvaszilas Sandstones samples of Aggtelek Mts. as well. Presumably the microbes
276 participated in the Fe-oxidation in this area too, but the amount of Fe-bearing fluid flow could be
277 low, and as a results did not form significant ore mineralization.

278 Concerning the source of Fe, the mafic rocks related to the Middle Triassic rifting represent
279 the most probable scenario, which also fits well with other areas (Brusnytsin & Zhukov 2012;
280 Maslennikov et al. 2012). The remnants of the mafic volcanism can be found in the Bódvavölgy

281 Ophiolite Formation (Fig. 4). This assumption fits well with the opinion of Szakáll (2001), that the
282 metasomatism related to the metamorphic fluids of the Middle Triassic (early Alpine) rifting. The
283 solution reacted with the sediments and sedimentary rocks in early diagenetic stage and according
284 to the different host (sediment and rock) effective microbial Fe-oxidation (enrichment) or
285 metasomatism and subordinate microbial Fe-oxidation occurred. Based on the spatial distribution
286 and the presence of the ore deposit in the succession, the ore formation went on during the early
287 diagenesis. The presence of the microbial signs at the cleavage plains of the creamspar and the
288 element distribution suggest that the sparite formation happened due to the metasomatism.
289 Consequently, the creamspar of Rudabánya was formed in an early diagenetic sediment by
290 microbial Fe-oxidation and metasomatism in proximal zone, while distal formation positions
291 include only traces of the same processes.

292 Considering the euhedral quartz megacrystals in creamspar, the concavo-convex grain contacts and
293 the syntaxial quartz overgrowths on monocrystalline quartz grains replacing the earlier creamspar,
294 the low $\delta^{13}\text{C}$ and $\delta^{18}\text{O}$ values and the thickness (more than 2000 meters) of the Lower Triassic –
295 Jurassic overlying formations, the succession was effected by deep burial diagenesis. According to
296 the low illite and chlorite crystallization values, the BSF later might have suffered
297 anchimetamorphism, nevertheless it needs further studies.

298

299 **6. Conclusions**

300

301 Mineralogical, petrographical and geochemical study of the Bódvaszilas Sandstone of the
302 Rudabánya open pit and the Aggtelek Mts. were summarized as part of the current iron and base
303 metal exploration in Rudabánya.

304 The composition and crystal structure of the historically identified „siliceous sparry iron
305 ore/creamspar” of Bódvaszilas Sandstone were determined for the first time, which is an
306 intermediate solid solution between siderite and magnesite.

307 In the lower section of the Triassic sequence, the pore-filling carbonate cement (creamspar) of the
308 Bódvaszilas Sandstone Formation was formed in the early stage of diagenesis by two-cycled
309 microbial Fe(II) mediation process. The creamspar in the higher parts of the formation (transition
310 between Bódvaszilas Sandstone and Szin Marl) was formed by the same metasomatic processes
311 producing the formerly exploited siderite in the Middle Triassic limestones and dolomites by the
312 partial or complete Fe replacement of the earlier carbonate layers.

313 Minor Fe addition may have occurred in Bódvaszilas Sandstone in the Aggtelek Mts, where the
314 pore-filling cement is also microbially mediated.

315 Considering the concavo-convex grain contacts and the syntaxial quartz overgrowths on
316 monocrystalline quartz grains, the formation underwent deep burial diagenesis, however, according
317 to the illite and chlorite crystallinity values the Bódvaszilas Sandstone might have suffered not only
318 (deep burial) diagenesis but at least anchimetamorphism both in the studied areas (Rudabánya,
319 Aggtelek Mts.).

320

321 **Acknowledgements**

322

323 The described work was carried out as part of the TÁMOP-4.2.2.A-11/1/KONV-2012-0005 project
324 as a work of Center of Excellence of Sustainable Resource Management, in the framework of the
325 New Széchenyi Plan, as well as with the support of Rotaqua Ltd. and the Geological and
326 Geophysical Institute of Hungary (Rákóczi-telep, core store).

327

328 **References**

- 329 Balla, L., Blitzer, Gy., Doszpoly, J., Harnos, J., Sóvágó, Gy., Szuromi, B., Varga, L. 1987. Iron ore
330 mining of Rudabánya, documentation of the closure of the mine, University of Miskolc,
331 Miskolc, 441 pp.
- 332 Bhatia, M.R. & Crook, K.A.W. 1986. Trace element characteristics of graywackes and tectonic
333 setting discrimination of sedimentary basins. *Contributions to Mineralogy and Petrology* 92,
334 181-193.
- 335 Brusnitsyn, A.I., Zhukov, I.G. 2012. Manganese deposits of the Devonian Magnitogorsk
336 palaeovolcanic belt (Southern Urals, Russia). *Ore Geology Reviews* 47, 42–58.
- 337 Csalagovits, I. 1973. Results of the geochemical and ore forming studies of the Triassic succession
338 in the Rudabánya area. *Annual report of the Hungarian Geological Society from 1971*, 61-
339 90.
- 340 Ehrlich, H.L., 1990. *Geomicrobiology*, 2nd ed. M. Dekker, New York (N.Y.). 719 pp.
- 341 Fodor, L., Csontos, L., Bada, G., Gyórfi, I., Benkovics, L. 1999. Tertiary tectonic evolution of the
342 Pannonian Basin system and neighbouring orogens: a new synthesis of paleostress data. In:
343 Durand, B., Joliver, L., Horváth, F., Séranne, M. (Eds.): *The Mediterranean Basins: Tertiary*
344 *extension within the Alpine Orogen*. Geological Society. Special Publications, London, 156,
345 298–334.
- 346 Fortin, D., Ferris, F.G., Beveridge, T.J., 1997, Surface-mediated mineral development by bacteria,
347 *in* Banfi eld, J., and Neelson, K.H., eds., *Geomicrobiology: Interactions between microbes*
348 *and minerals: Mineralogical Society of America Reviews in Mineralogy Volume 35*, p. 162–
349 180.
- 350 Földessy, J., Németh, N., Gerges, A. 2010. Preliminary results of the re-exploration of the
351 Rudabánya base metal ore deposit. *Bulletin of the Hungarian Geological Society*, 140, 3,
352 281–292. (in Hungarian)
- 353 Fügedi, U., Szentpétery, I., Chikán, G., Vatai, J. 2010: The Rudabánya-Martonyi mineralisation:
354 possible geochemical reconstruction. *Carpathian Journal of Earth and Environmental*
355 *Sciences* 5/2, 81–88.
- 356 Hernyák, G., 1967. Siliceous siderite and hematite in the Lower Triassic (Seis) of Rudabánya (NE-
357 Hungary). *Földtani kutatás*. 10, 1, 1-6. (in Hungarian)
- 358 Hofstra, A.H., Korpás, L., Csalagovits, I., Johnson, C.A. & Christiansen, W.D. 1999. Stable
359 isotopic study of the Rudabánya iron mine, a carbonate-hosted siderite, barite, base-metal
360 sulfide replacement deposit. *Geologica Hungarica, Series Geologica* 24, 295–302. (in
361 Hungarian)

- 362 Hurai, V. 2005. "Siderite mineralization of the Gemericum superunit (Western Carpathians,
363 Slovakia): review and a revised genetic model" [Ore Geology Reviews 24, 267–298]—a
364 discussion. – Ore Geology Reviews 26, 167–172.
- 365 Konhauser, K. O. 1998: Diversity of bacterial iron mineralization. – Earth-Science Reviews 43, 91–
366 121.
- 367 Kovács, S., Less, Gy., Hips, K., Piros, O., Józsa, S. 2004: Aggtelek-Rudabánya units, in: Haas, J.
368 (ed.): Geology of Hungary. Triassic, ELTE Eötvös Kiadó, Budapest, 197-216. (in
369 Hungarian)
- 370 Less, Gy., Grill, J., Gyuricza, Gy., Róth, L., Szentpétery, I. 1988: 1:25000 scale geological map of
371 the Aggtelek-Rudabánya Mts., Hungarian Geological Institute, Budapest (in Hungarian)
- 372 Maslennikov, V.V., Ayupova, N.R., Herrington, R.J., Danyushevskiy, L.V., Large, R.R. 2012:
373 Ferruginous and manganiferous haloes around massive sulphide deposits of the Urals. – Ore
374 Geology Reviews 47, 5–41.
- 375 Nagy, B. 1982. The comparative ore forming study of the Rudabánya ore deposit. Annual report of
376 the Hungarian Geological Society from 1980, p. 45–58.
- 377 Németh, N., Földessy, J., Kupi, L. & Iglesias, J.G. 2013. Zn-Pb mineralization types in the
378 Rudabánya ore bearing complex. Carpathian Journal of Earth and Environmental Sciences,
379 8, 1, 47–58.
- 380 Palinkaš, L. A., Šoštarić, S. B., Palinkaš, S. S. 2008: Metallogeny of the Northwestern and Central
381 Dinarides and Southern Tisia. Ore Geology Reviews 34, 501–520.
- 382 Pantó, G. 1956. Geology of the Rudabánya iron ore ridge. Yearbook of the Hungarian Geological
383 Institute, 44, 2, 329–637. (in Hungarian)
- 384 Rimmer, S. 2004. Geochemical paleoredox indicators in Devonian–Mississippian black shales,
385 Central Appalachian Basin (USA). Chemical Geology 206, 373–391.
- 386 Scholle, P. A. & Ulmer-Scholle, D. S. 2003. A color guide to the petrography of carbonate rocks:
387 grains, textures, porosity, diagenesis, AAPG Memoir 77, Tulsa (Oklahoma, U.S.A.), p. 459.
- 388 Schwertmann, U., Cornell, R.M., 2007. Iron Oxides in the Laboratory: Preparation and
389 Characterization, Wiley-VCH, p. 188.
- 390 Szakáll, S. 2001. The Minerals of Rudabánya. Köország Kiadó, Budapest, p. 176. (in Hungarian)
- 391 Szentpétery I. & Less Gy. (Eds.) 2006. Geology of the Aggtelek-Rudabánya Mts. Explanations to
392 the 1:25000 scale geological map of the Aggtelek-Rudabánya Mts. published in 1986.
393 Hungarian Geological Institute, Budapest, p. 92. (in Hungarian)

- 394 Yang, B., Hu, B., Bao, Z., Zhang, Z. 2011. RFF geochemical characteristics and depositional
395 environment of the black shale-hosted Baiguoyuan Ag-V deposit in Xingshan, Hubei
396 Province, China. *Journal of Rare Earths* 29/5, 499–506.
- 397 Wignall, P.B., Myers, K.J. 1988. Interpreting the benthic oxygen levels in mudrocks: a new
398 approach. *Geology* 16, 452–455.
- 399

400 **Figure captions**

401 **Fig. 1.**

- 402 (a) Location of the Rudabánya iron and base metal deposit in the Alp-Carpathian region (after
403 Fodor et al., 1999)
404 (b) The Rudabánya research area and the sampling points of Bódvaszilas Sandstone Formation
405 (c) Geological section of Rudabánya ore deposit (after Less et al. 1988)

406 **Fig. 2.**

- 407 (a) Filamentous, pearl necklace-like mineralized microbially produced texture (MMPT) in pore-
408 filling carbonate cement (Rudabánya)
409 (b) Filamentous textures (MMPT) along the cleavage faces of the sparite crystals in the massive
410 carbonate sections (Rudabánya)
411 (c) Filamentous, pearl necklace-like MMPT in pore-filling carbonate cement (Aggtelek Mts.)
412 (d) Green clay minerals between the grains of Bódvaszilas Sandstone
413 (e) Texture of pore-filling creamspar by EPMA (Q – quartz grains, Si – siderite, Mg – magnesite)
414 (f) Texture of pore-filling creamspar by optical microscopy (Q – quartz grains, arrows: MMPT)

415 **Fig. 3.** Composition of creamspar samples on the Fe-Mg-Mn diagram

- 416 **Fig. 4.** The evolution of the Lower Triassic Bódvaszilas Sandstone according to this study
417 (Geological section after Szentpétery & Less Gy. 2006)

Table 1. Geochemical environmental indicators of some representative samples of Bódvaszilás Sandstone

Sample	Th/U	U/Th	δU	V/Cr	Ni/Co
BH/1	5.41	0.18	-0.85	1.15	0.33
T11/3	4.78	0.21	-1.50	1.30	3.57
T11/4	4.76	0.21	-1.47	1.14	2.89
T11/6	5.44	0.18	-2.94	0.59	2.00
T14A/4	3.32	0.30	-0.13	3.20	2.00
T14A/5	5.16	0.19	-2.03	1.05	4.67

Figure

[Click here to download high resolution image](#)

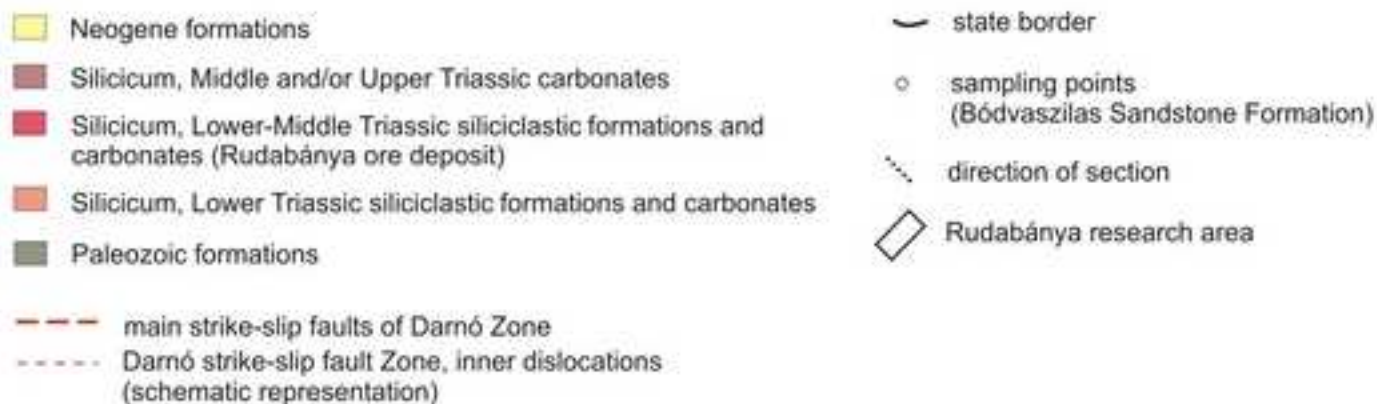
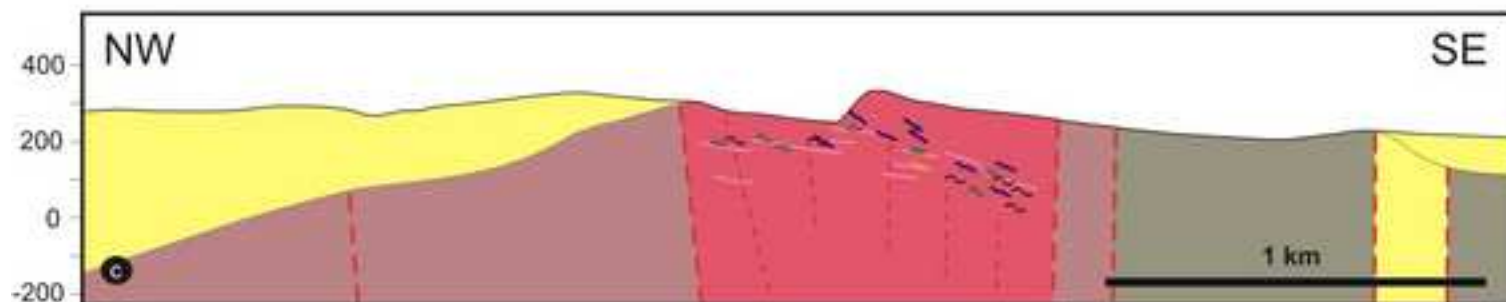
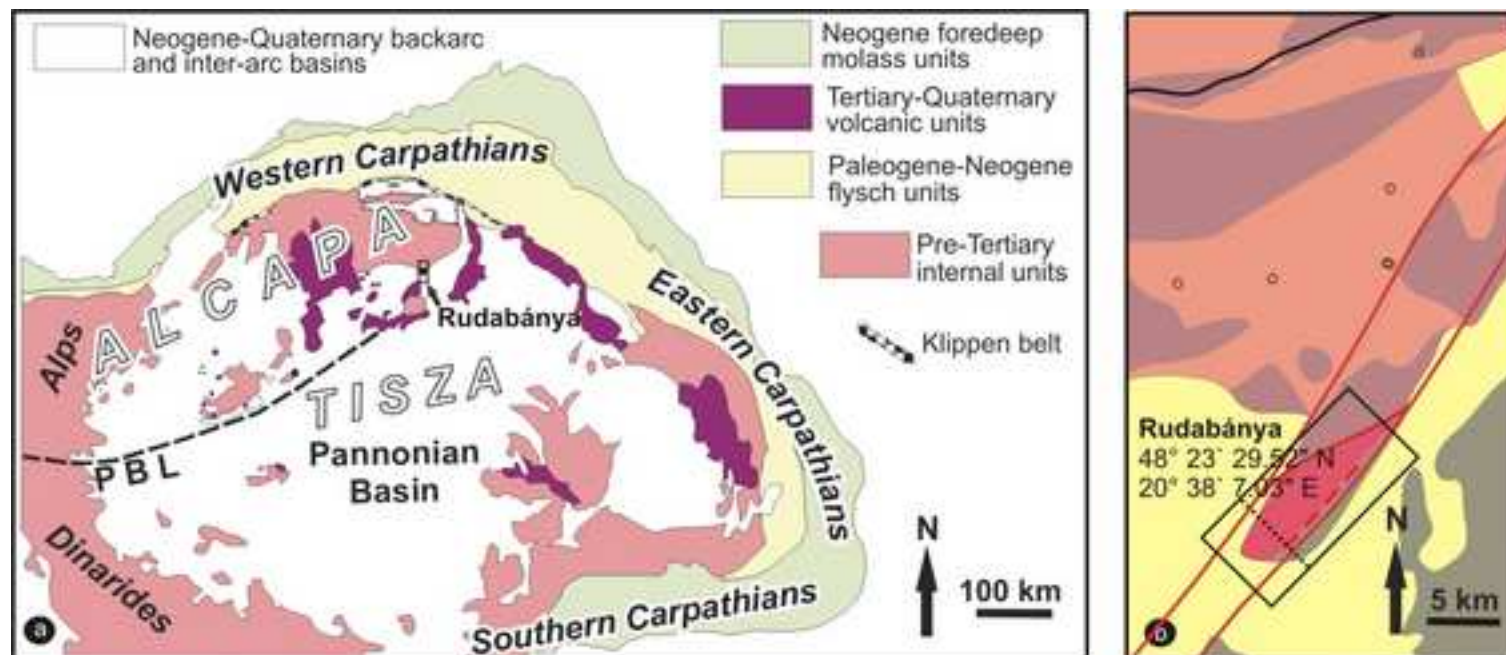


Figure
[Click here to download high resolution image](#)

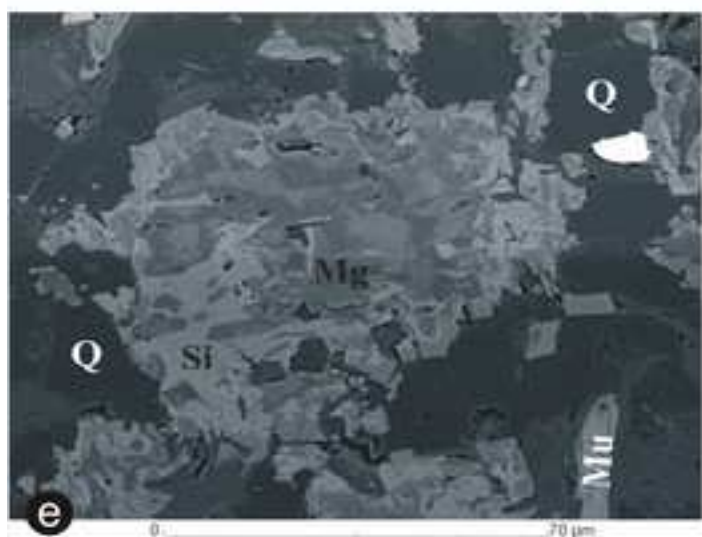
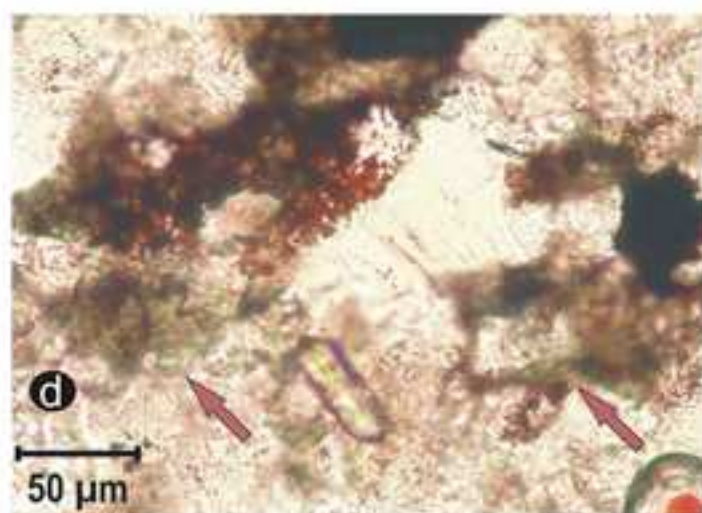
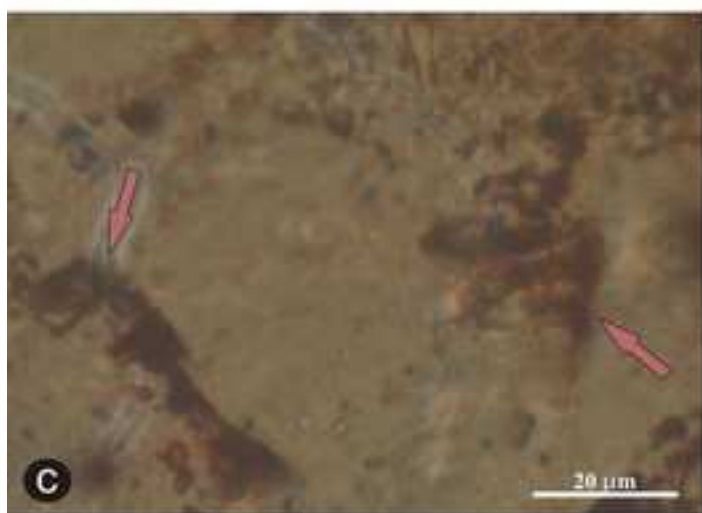
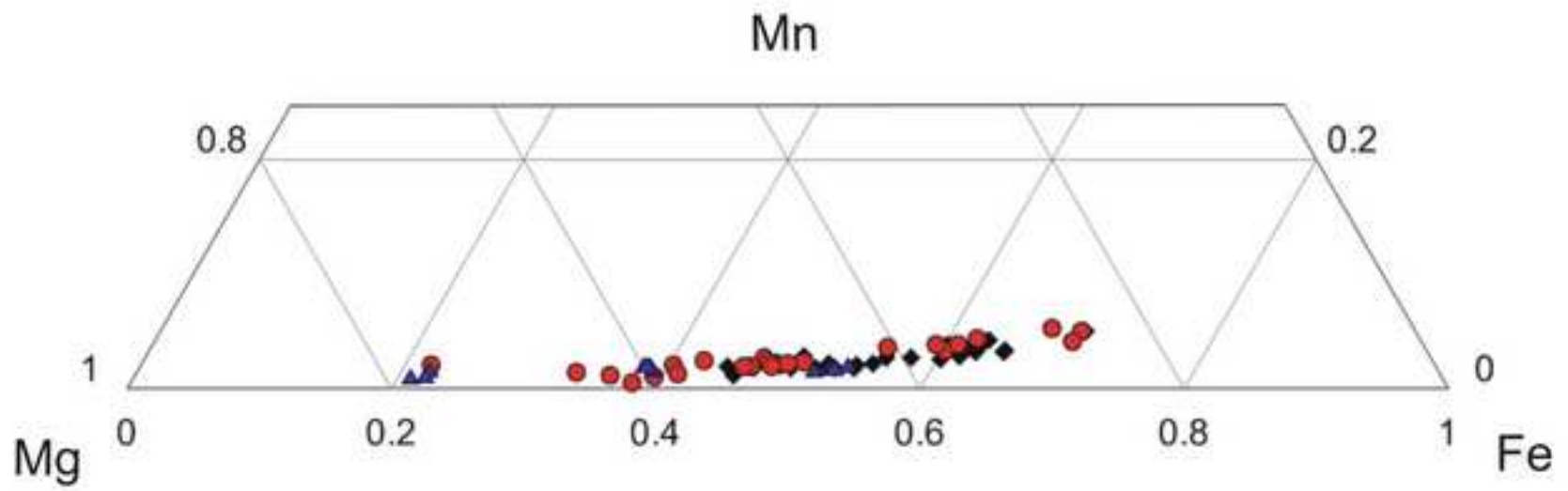


Figure
[Click here to download high resolution image](#)



Figure

[Click here to download high resolution image](#)

